Voltage-gated Sodium Channel Activity Promotes Cysteine Cathepsin-dependent Invasiveness and Colony Growth of Human Cancer Cells

Ludovic Gillet, Sébastien Roger, Pierre Besson, Fabien Lecaille, Jacques Gore, Philippe Bougnoux, Gilles Lalmanach, Jean-Yves Le Guennec

Voltage-gated Sodium Channel Activity Promotes Cysteine Cathepsin-dependent Invasiveness and Colony Growth of Human Cancer Cells*[S]

Ludovic Gillet[‡1,2], **Sébastien Roger**[‡1,3], **Pierre Besson**[‡], **Fabien Lecaille**[§], **Jacques Gore**[‡], **Philippe Bougnoux**[‡], **Gilles Lalmanach**[§], **and Jean-Yves Le Guennec**[‡]

From [‡]INSERM U921, Nutrition, Croissance et Cancer, and [§]INSERM U618, Protéases et Vectorisation Pulmonaires, Université François Rabelais, Faculté de Médecine, 37032 Tours, France

Voltage-gated sodium channels (Na$_V$) are functionally expressed in highly metastatic cancer cells derived from nonexcitable epithelial tissues (breast, prostate, lung, and cervix). MDA-MB-231 breast cancer cells express functional sodium channel complexes, consisting of Na$_V$1.5 and associated auxiliary β-subunits, that are responsible for a sustained inward sodium current at the membrane potential. Although these channels do not regulate cellular multiplication or migration, their inhibition by the specific blocker tetrodotoxin impairs both the extracellular gelatinolytic activity (monitored with DQ-gelatin) and cell invasiveness leading to the attenuation of colony growth and cell spreading in three-dimensional Matrigel®-composed matrices. MDA-MB-231 cells express functional cysteine cathepsins, which we found play a predominant role (~65%) in cancer invasiveness. Matrigel® invasion is significantly decreased in the presence of specific inhibitors of cathepsins B and S (CA-074 and Z-FL-COCHO, respectively), and co-application of tetrodotoxin does not further reduce cell invasion. This suggests that cathepsins B and S are involved in invasiveness and that their proteolytic activity partly depends on Na$_V$ function. Inhibiting Na$_V$ has no consequence for cathepsins at the transcription, translation, and secretion levels. However, Na$_V$ activity leads to an intracellular alkalinization and a perimembrane acidification favorable for the extracellular activity of these acidic proteases. We propose that Na$_V$ enhance the invasiveness of cancer cells by favoring the pH-dependent activity of cysteine cathepsins. This general mechanism could lead to the identification of new targets allowing the therapeutic prevention of metastases.

Breast cancer is the most common female cancer and the primary cause of death in women by cancer worldwide (1).

Deaths occur primarily after the development of metastases. The invasive potential of malignant cells is mainly linked to their capacity to degrade basement membranes and extracellular matrices by various proteases. Studies have mostly focused on metalloproteases, including matrix metalloproteinases and the closely related ADAMs (a disintegrin and metalloproteinase) and ADAMTs (a disintegrin and metalloproteinase with thrombospondin motifs) (2), that are key factors in growth, invasion, and angiogenesis, and to a lesser extent on aspartyl and serine proteases. Pharmaceutical inhibitors of matrix metalloproteinases have been developed, but the results from clinical trials with these drugs have so far been disappointing (3, 4). On the other hand, cysteine cathepsins (Cat)[4] related to papain (family C1, clan CA), which have been confined for decades to housekeeping tasks including intracellular degradation of endocytosed proteins (5), are now known to fulfill more specific functions in numerous biological processes (such as antigen presentation, enzyme or hormone maturation, bone resorption, etc.) and pathologies (6, 7). Recently, they have emerged as important protagonists in cancer and have been reported to be involved in apoptosis, angiogenesis, proliferation, migration, and invasion (8–10). Although Cat are predominantly expressed in acidic endosomal/lysosomal compartments, they are also found to be extracellularly active at physiological pH, as membrane-bound and soluble forms (11–14). Nevertheless knowledge still remains limited concerning transport pathways and regulation of extracellular Cat in cancer cells.

The involvement of ion channels in carcinogenesis and tumor progression begins to be unraveled even though their roles are not totally understood. Presently, there is growing evidence emphasizing the abnormal expression and function of voltage-gated sodium channels (Na$_V$) in cancer cells and their involvement in invasiveness (15). Indeed, Na$_V$, which are up-regulated in human breast cancer tissues and associated with breast cancer progression, are functionally expressed in the highly metastatic MDA-MB-231 breast cancer cells in which

they potentiate invasion (16, 17). This makes MDA-MB-231 cells a good model for studying the specific molecular mechanisms linking the activity of Na$_V$ to invasive properties of cancer cells. In this context, the aim of the present study was to identify, among proteolytic enzymes involved in cancer cell invasion, those that are regulated by Na$_V$ activity. We demonstrated that Cat are the predominant proteases involved in MDA-MB-231 invasiveness and that the activity of Na$_V$ favors the pericellular activity of CatB and CatS, through the acidification of the perimembrane pH. We also performed experiments in non-small cell lung cancer cells (H460 cell line), which also express functional Na$_V$ involved in cellular invasiveness (18). Similar results were obtained, highlighting the fact that Cat are partly regulated by Na$_V$ activity. This work presents a new general mechanism for highly metastatic cancer cell invasiveness.

EXPERIMENTAL PROCEDURES

Inhibitors, Substrates, and Chemicals—Tetrodotoxin (TTX) was purchased from Latoxan (France) and was prepared in pH-buffered physiological saline solution at pH 7.4. Fluorescent dyes for measuring internal and perimembrane pH (BCECF-AM and DHPE, respectively) were purchased from Invitrogen (France). Protease inhibitors and substrates were purchased from Calbiochem (VWR International). The cell-impermeant Cat inhibitors are: E-64 (100 μM), a broad spectrum inhibitor (19), CA-074 (L-3-trans-(propylcarbamoyl)oxirane-2-carbonyl)-L-isoleucyl-L-proline, 25 nM), a CatB inhibitor (20), N-(4-biphenylacetyl)-S-methylcysteine-(D)-Arg-Phe-β-phenethylamide, 200 nM), a CatL inhibitor (21), Z-L-NHNH-CONHNH-LF-Boc (1-(N-benzyloxycarbonyl-leucyl)-5-(N-Boc-phenylalanyl-leucyl)carbohydrazide, 100 nM), a CatK inhibitor (22), and Z-Phe-Leu-COCHO (2 nM), a slow, tight binding inhibitor of CatS (23). Fluorogenic substrates were Z-Phe-Arg-AMC (Z-FR-AMC), Z-Arg-Arg-AMC (Z-RR-AMC), Z-Leu-Arg-AMC (Z-LR-AMC), and Z-Gly-Pro-Arg-AMC (Z-GPR-AMC). Other drugs and chemicals were purchased from Sigma-Aldrich.

Cancer Cell Culture and Colony Growth—The cancerous human cell lines, MDA-MB-231 (breast) and H460 (lung) were purchased from the ATCC and cultured in Dulbecco's modified Eagle's medium (DMEM; Cambrex) supplemented with 5% fetal calf serum. When indicated, MDA-MB-231 cells were seeded on a planar film or in a three-dimensional matrix of Matrigel®. Experiments assessing the involvement of Na$^+$ in the invasion process were performed in "Normo Na" and in "Low Na" culture media. These culture solutions were prepared from a DMEM solution (Cambrex) deprived of NaCl, KCl, and CaCl$_2$. The Normo Na solution was prepared by adding 5.4 mM KCl, 2 mM CaCl$_2$, and 110 mM NaCl. The Low Na solution was prepared by adding the same salts as above except that NaCl was replaced by 110 mM choline chloride. Under these conditions, the total concentrations of Na$^+$ are, respectively, 155 and 45 mM (45 mM of Na$^+$ being supplied in both conditions by 44 mM NaHCO$_3$ and 1 mM NaH$_2$PO$_4$). These solutions were then supplemented with 5% fetal calf serum. Cell size, number, and size of colonies, and the number of cells spreading into the three-dimensional matrix were analyzed with the ImageJ software 1.38I (National Institutes of Health). The assessment of

sizes for cells and cell colonies was done by evaluating cell surface from pictures coming from separate experiments. The numbers of colonies and cells were counted from pictures.

Electrophysiology—Patch pipettes were pulled from borosilicate glass to a resistance of $4-6$ MΩ. Currents were recorded, in whole cell configuration, under voltage clamp mode at room temperature using an Axopatch 200 B patch clamp amplifier (Axon Instruments). Analogue signals were filtered at 5 kHz and sampled at 10 kHz using a 1322A Digidata converter. Cell capacitance and series resistance were electronically compensated by about 60%. The P/2 subpulse correction of cell leakage and capacitance was used to study Na$^+$ current (I_{Na}). Sodium currents were recorded by depolarizing the cells from a holding potential of -100 mV to a maximal test pulse of -5 mV for 30 ms every 500 ms. The protocol used to build sodium current-voltage (I_{Na}-V) relationships was as follows: from a holding potential of -100 mV, the membrane was stepped to potentials from -90 to $+60$ mV, with 5-mV increments, for 50 ms at a frequency of 2 Hz. Availability-voltage relationships were obtained by applying 50-ms prepulses using the I_{Na}-V curve procedure followed by a depolarizing pulse to -5 mV for 50 ms. In this case, the currents were normalized to the amplitude of the test current without a prepulse. Conductance through Na$^+$ channels (g_{Na}) was calculated as already described (17). The current amplitudes were normalized to cell capacitance and expressed as current density (pA/pF).

The physiological saline solution (PSS) had the following composition: 140 mM NaCl, 4 mM KCl, 1 mM MgCl$_2$, 2 mM CaCl$_2$, 11.1 mM D-glucose, and 10 mM HEPES, adjusted to pH 7.4 with NaOH (1 M). The intrapipette solution had the following composition: 125 potassium glutamate, 20 mM KCl, 0.37 mM CaCl$_2$, 1 mM MgCl$_2$, 1 mM Mg-ATP, 1 mM EGTA, 10 mM HEPES, adjusted to pH 7.2.

Assessment of Gelatinolytic Activity by Confocal Microscopy—MDA-MB-231 cells were cultured in a three-dimensional Matrigel® matrix containing 25 μg/ml of DQ-Gelatin® (Invitrogen) on glass coverslips for 24 h and were then fixed for 10 min in 4% paraformaldehyde in phosphate-buffered saline at room temperature. Confocal microscopy was performed with an Olympus Fluoview 500 instrument. The samples were excited at 495 nm, and emission light was recorded at 515 nm. Fluorescence density was quantified by image analysis thanks to the ImageJ software 1.38I.

Cell Survival and Proliferation—The cells were seeded at 4×10^4 cells/well in a 24-well plate coated or not with Matrigel® and were grown for a total of 5 or 6 days. The culture medium and TTX and/or Cat inhibitors were changed every other day. Growth and viability of cells were measured as a whole by the tetrazolium salt assay (24) as previously described (17). Viable cell number was assessed at 570 nm (formazan absorbance) and normalized to the control condition, without TTX (on the same day of the experiment).

Migration and in Vitro Invasion Assay—Migration was analyzed in 24-well plates receiving 8-μm pore size polyethylene terephtalate membrane cell culture inserts (BD Biosciences). The upper compartment was seeded with 4×10^4 cells in DMEM supplemented with 5% fetal bovine serum. The lower compartment was filled with DMEM supplemented with 10% fetal bovine serum,
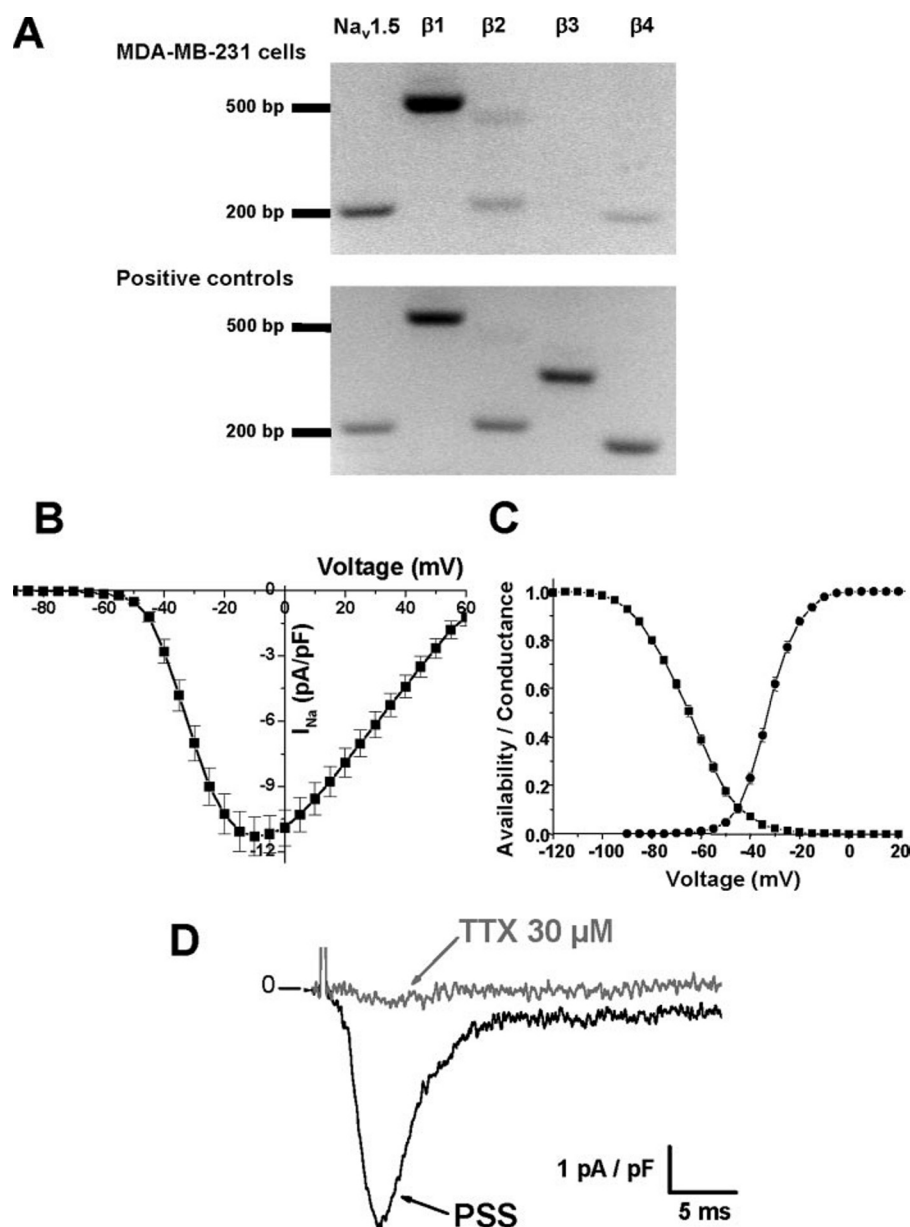
FIGURE 1. **Characterization of Na$_V$ in breast cancer cells.** *A*, reverse transcription-PCR experiments showing the mRNA expression of the Na$_V$1.5 α-subunit and of the β1, β2, and β4 subunits in MDA-MB-231 breast cancer cells. This figure is representative of four separate experiments. *B*, current-voltage relationship of the sodium current obtained from a holding potential of -100 mV ($n = 80$ cells). *C*, conductance ($\bullet$) and availability ($\blacksquare$) voltage relationships obtained in the same cells as in *B*. *D*, effect of 30 μM TTX on a current elicited by a depolarization to -30 mV from a holding potential of -100mV.

Cell Line RNA Extraction, Reverse Transcription, Quantitative, and Conventional PCR—Total RNA extraction from MDA-MB-231 cells was performed by using RNAgents® total RNA isolation system (Promega). RNA yield and purity were determined by spectrophotometry, and only samples with an A_{260}/A_{280} ratio above 1.6 were kept for further experiments. Total RNA were reverse-transcribed with the RT kits Ready-to-go® You-prime First-Strand Beads (Amersham Biosciences). Random hexamers pd(N)$_6$ 5'-Phosphate (0.2 μg; Amersham Biosciences) were added, and the reaction mixture was incubated at 37 °C for 60 min. Quantitative (real time) PCR experiments were performed with an iCycler™ system (Bio-Rad). The PCR protocol consisted of a denaturation step at 95 °C for 2 min, followed by 35 cycles of amplification at 95 °C for 15 s, 60 °C for 30 s, and 72 °C for 10 s. The experiments were performed in triplicate, and negative controls containing water instead of first strand cDNA were done. The results were calculated with the ΔC_t method, where the parameter C_t (threshold cycle) is defined as the fractional cycle number at which the PCR reporter signal passes a fixed threshold. For each sample ΔC_t values were determined by subtracting the average C_t value of the investigated transcript under control conditions (cells grown in normal culture medium) from the average C_t value of the same transcript when the cells were grown for 24 h in presence of 30 μM TTX. For conventional PCR, the temperature profile was 2 min at 94 °C, followed

as a chemoattractant. After 24 h at 37 °C, the remaining cells were removed from the upper side of the membrane. The cells that had migrated and were attached to the lower side were stained with hematoxylin and counted in the whole insert, using a light microscope (200× magnification). *In vitro* invasion was assessed using the same inserts and the same protocol as above but with the membrane covered with a film of Matrigel® (extracellular-mimicking matrix; BD Biosciences). Migration and invasion assays were performed in triplicate in eight separate experiments. For easier comparison between cells lines, the results obtained for migration and invasion were normalized to the control condition. In addition, invasion experiments were repeated in Normo Na$^+$ (155 mM) or in Low Na$^+$ solutions (45 mM).

by 35 cycles of amplification which consisted of 30 s of DNA denaturation at 94 °C, 60 s of primers hybridization at 60 °C, and 20 s of polymerization at 72 °C and a final extension for 2 min at 72 °C. PCR products were then analyzed by electrophoresis in a 2% agarose gel containing ethidium bromide and visualized by UV trans-illumination (Gel Doc 2000 system; Bio-Rad). Primers used for PCR experiments had the following sequences (expected sizes): Na$_V$1.5, forward 5'-CACGCGTT-CACTTTCCTTC-3' and reverse 5'-CATCAGCCAGCTTCT-TCACA-3' (208 bp); β1, forward 5'-GAAAACTACGAGCAC-AACACCA-3' and reverse 5'-GGCAGTATTGCTTTACCC-ATCA-3' (510 bp); β2, forward 5'-TGACCCACTCTCTTCC-ATCC-3' and reverse 5'-GGTCCTCTCTGAAGCCACTG-3'
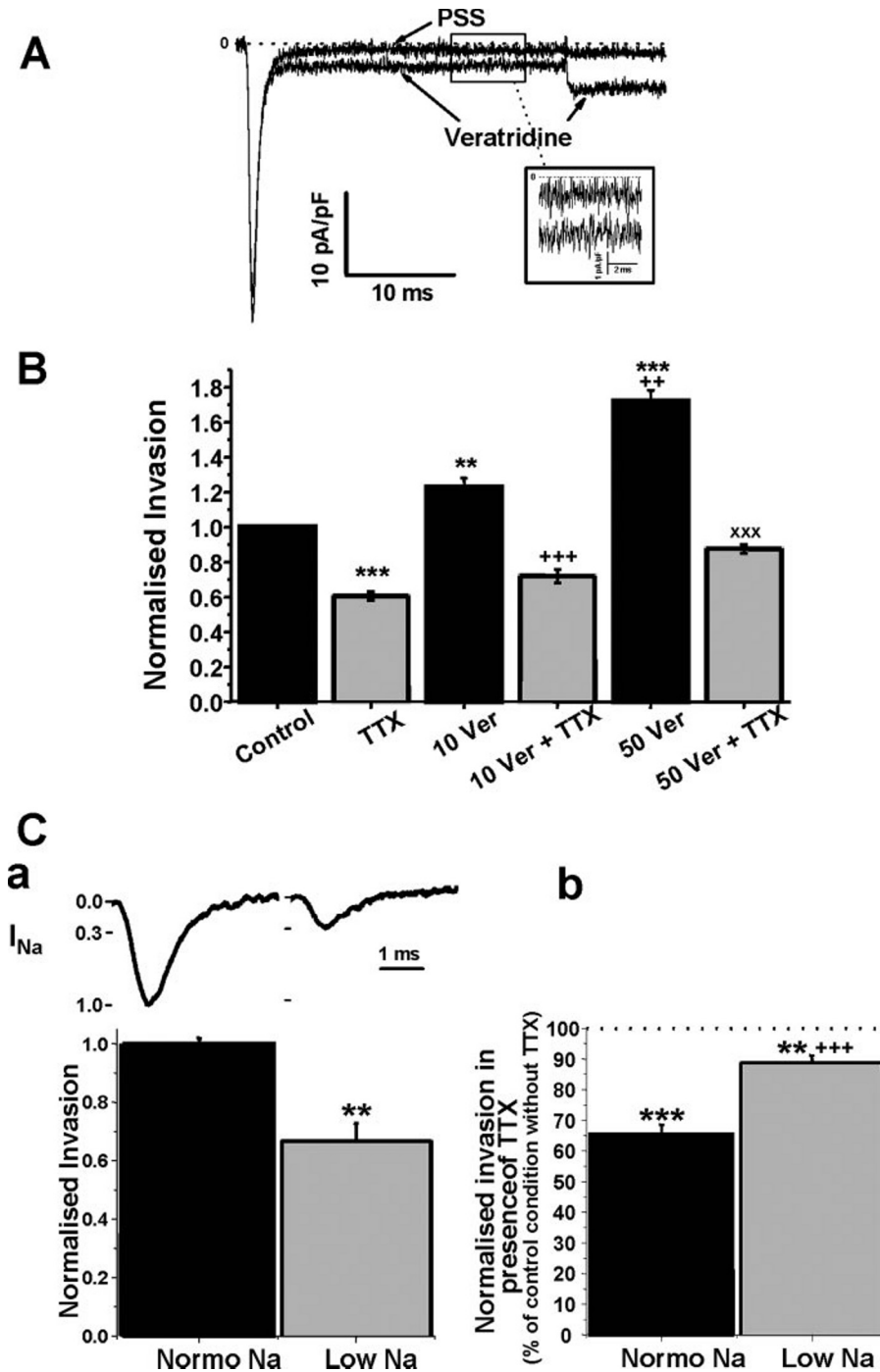
FIGURE 2. **Involvement of the sodium influx through Na_V in invasion.** *A*, effect of veratridine (50 μM) on a sodium current elicited by a depolarization to -5 mV from a holding potential of -100 mV. The *inset* emphasizes the veratridine-induced increase of the sustained current. *B*, effect of 30 μM TTX, alone or in combination with veratridine (*Ver*, 10 or 50 μM), on the MDA-MB-231 human breast cancer cells invasion. Statistically different: *, *versus* control condition; +, *versus* veratridine 10 and $\times$, *versus* veratridine 50 ($n = 8$ separate experiments). *C*, effect of external Na$^+$ on MDA-MB-231 invasion. *Panel a*, effect of reducing external Na$^+$ in culture medium, from 155 mM (*Normo Na*) to 45 mM (*Low Na*), on cell invasion ($n = 4$ separate experiments). Above each *bar* is shown the corresponding sodium current elicited from a holding potential of -100 to -5 mV in both external solutions (DMEM Normo Na and Low Na). *Panel b*, effect of TTX on cell invasion as a function of the extracellular culture medium: Normo Na or Low Na. Statistically different: *, *versus* control condition in absence of TTX; +, *versus* Normo Na condition (one symbol for $p < 0.05$; two symbols for $p < 0.01$, and three symbols for $p < 0.001$).

(188 bp); CatB, forward 5′-ACAGC-CCGACCTACAAACAG-3′ and reverse 5′-CCAGTAGGGTGTGCC-ATTCT-3′ (239 bp); CatS, forward 5′-TCTCTCAGTGCCCAGAA-CCT-3′ and reverse 5′-GCCACA-GCTTCTTTCAGGAC-3′ (248 bp); CatK, forward 5′-CCTTGAGGCT-TCTCTTGGTG-3′ and reverse 5′-GGGCTCTACCTTCCCATTCT-3′ (134 bp); CatL, forward 5′-AGGAGAGCAGTGTGGGAGAA-3′ and reverse 5′-TGGGCTTACG-GTTTTGAAAG-3′ (160 bp); Cystatin C, forward 5′-GATCGTAGC-TGGGGTGAACT-3′ and reverse 5′-CCTTTTCAGATGTGGCTGGT-3′ (115 bp); Cystatin M, forward 5′-CTTCCTGACGATGGAGATGG-3′ and reverse 5′-GGAACCACAA-GGACCTCAAA-3′ (141 bp); and Stefin B, forward 5′-TAGGAGAG-CGTGGCTGTTTT-3′ and reverse 5′-TGATGCTCCCTCTTCTGTCC-3′ (128 bp). The efficacy of the primers for Na$_V$1.5 and β-subunits was checked in human tissues where the various isoforms are known to be expressed, *i.e.* in cardiac muscle for Na$_V$1.5 and in the central nervous system for β1 to β4.

siRNA Transfection Protocol—MDA-MB-231 breast cancer cells were transfected with siRNA directed against SCN5A mRNA (siNa$_V$1.5) or scramble siRNA-A as a control (siCTL), which were purchased from Santa Cruz, Tebu-Bio (France). Briefly, cells in suspension were transfected with 20 nM siRNA by using Lipofectamine RNAi max (Invitrogen). The experiments (invasion assays and patch clamp) were performed 24 h after transfection.

Fluorescence Measurement of Intracellular pH and Perimembrane pH—Intracellular and perimembrane pH were measured using ratiometric methods (Cairn Optoscan) with BCECF (excitation, 400/490 nm; emission, 535 nm) and fluorescein DHPE (excitation, 440/485 nm; emission, 535 nm)

respectively. The cells were incubated for 45 min at room temperature in PSS containing 5 μM BCECF-AM. Perimembrane pH was monitored by incubating the cells with 1 μg/ml of fluorescein DHPE in serum-free DMEM for 1 h at
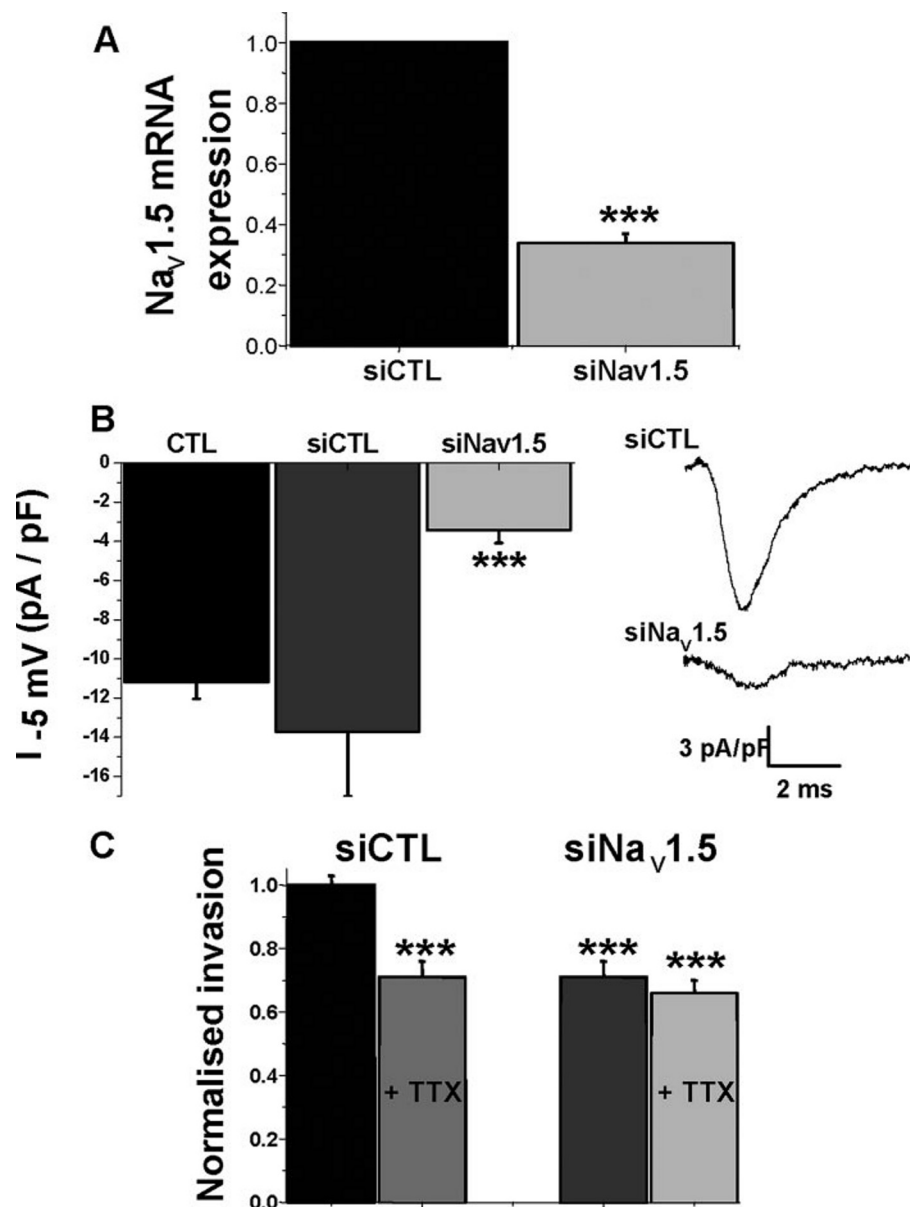
(216 bp); β3, forward 5′-TCAACGTCACTCTGAACGA-CTC-3′ and reverse 5′-CATGTCACACTGCTCCTGT-TCT-3′ (346 bp); β4, forward 5′-ACAGCAGTGACGCATTC-AAG-3′ and reverse 5′-CACATGGCAGGTGTATTTGC-3′

FIGURE 3. **Effect of transcriptional disruption of Na$_V$ channels in MDA-MB-231 cells, using 20 nM siRNA against Na$_V$1.5 (siNa$_V$1.5) *versus* control (siCTL).** *A*, Na$_V$1.5 mRNA expression assessed by Q-PCR ($n = 2$ experiments). *B*, Na$_V$1.5 currents recorded at -5 mV from a holding potential of -100 mV in untransfected cells (*CTL*, $n = 80$) or in cells transfected with 20 nM control siRNA (siCTL, $n = 10$) or siRNA against Na$_V$1.5 (siNa$_V$1.5, $n = 17$). Representative currents elicited by a depolarization from -100 mV to -5 mV, recorded from non-transfected cells (*CTL*), siCTL, or siNa$_V$1.5 transfected cells, are shown on the *right*. *C*, Matrigel® invasion by cells transfected with siCTL or siNa$_V$1.5 and treated or not with 30 μM TTX, normalized to siCTL without TTX treatment ($n = 4$ separate experiments). The values are statistically different at $p < 0.001$ when compared with siCTL (*A–C*) or CTL (*B*).

lysed in presence of radioimmunoprecipitation assay lysis buffer (50 mM Tris-HCl, pH 7.5, 150 mM NaCl, 1% Nonidet P-40, 0.25% sodium deoxycholate, 1 mM EDTA), containing 1% Triton X-100 and protease inhibitors (Complete; Roche Applied Science) for 1 h at 4 °C. Cell lysates were centrifuged at 16,000 × g for 10 min to remove insoluble debris. Total proteins concentrations were determined using the bicinchoninic acid method (Bio-Rad). Alternatively, culture media from cells cultivated on a Matrigel® basement membrane were centrifuged to remove floating cells and then concentrated by centrifugation with Amicon Ultra-4 columns (Millipore) at 4,000 × g for 30 min. Protein samples were diluted in the sample buffer under reducing conditions, boiled for 3 min, separated by SDS-PAGE on 12% gels (25), and then transferred onto a polyvinylidene difluoride membrane (Millipore). After saturation for 2 h in 5% nonfat milk Tris-buffered saline solution containing 0.5% Tween 20 (TTBS), the membrane was incubated overnight at 4 °C with the primary antibody (1/1,000) in a 2% nonfat milk TTBS solution. The membrane was further incubated for 1 h at room temperature, with a goat anti-rabbit (1/6,000) horseradish peroxidase-conjugated secondary antibody (Santa Cruz Biotechnology). ECL (Amersham Biosciences) was used for immunodetection. Densitometric analyses were performed using QuantityOne software v4.6.3 (Bio-Rad).

Cathepsin Activity Assays—After growing MDA-MB-231 cells on Matrigel®-coated flasks, total cell extracts were obtained by a series of

37 °C. In both cases, excess dye was removed by rinsing the cells twice with PSS.

Calibration for each dye was performed by perifusing each studied cell with varying pH (pH 6.9–7.6). For determining internal pH, 0.01 mM nigericin was added to the solution. All of the data were corrected for background fluorescence.

Western Blots—The specific primary antibodies were rabbit anti-human Cat B (Fitzgerald) and cathepsin S, K, and L (Calbiochem). MDA-MB-231 cells in their subconfluent state cultivated on a Matrigel® basement membrane were washed twice with phosphate-buffered saline. The cells were scraped and

seven freeze/thaw cycles in liquid nitrogen and a 30 °C water bath. Concentrated supernatants were prepared as described above. For the assessment of membrane-associated Cat activity, the cells were scraped in phosphate-buffered saline. A panel of AMC-derived fluorogenic substrates were used to measure proteolytic activities. The activation buffer was 0.1 M sodium acetate buffer, pH 5.5, containing 2 mM EDTA and 2 mM dithiothreitol. After activation for 5 min, kinetic measurements were continuously recorded with a microtiter plate reader at 30 °C with $\lambda_{ex} = 350$ nm and $\lambda_{em} = 460$ nm (Gemini spectrofluorimeter; Molecular Devices). The activities of CatB/K/

L/S were measured using Z-FR-AMC (10 μM), that of CatB using Z-RR-AMC (10 μM), those of CatK/S (K > S > L) were measured using Z-LR-AMC (10 μM), and those of CatK/B (K $\gg$ B) were measured using Z-GPR-AMC (10 μM). Experiments with Z-FR-AMC were also performed at pH 8.0 in a Tris-HCl buffer containing 2 mM EDTA and 2 mM dithiothreitol. Specificity of the Cat-dependent hydrolysis was checked by preincubation with E-64 (100 μM). Measurement of the overall Cat activity in concentrated supernatants was performed using Z-FR-AMC (25 μM) after 2 h of incubation at 30 °C at pH 5.5 in acetate buffer in presence of dextran sulfate (40 μg/ml). Total Cat were titrated by using increasing concentrations of E-64 (0–50 nM). The same experiment was repeated in the presence of CA-074 (0–25 nM) for titration of CatB.

Statistical Analyses—The data are displayed as the means $\pm$ S.E. of the mean (n = number of cells/experiments). One-way analysis of variance on ranks followed by a Student-Newmann-Keul's test were used to compare cell proliferation, migration and invasion, secretion of Cat, and intracellular and perimembrane pH in control conditions or in the presence of the different drugs and inhibitors. t tests were used to compare cell numbers, colony numbers and sizes, and the number of cells escaping from colonies. Alternatively, a Mann-Whitney rank sum test was used when the variance homogeneity test failed. Statistical significance is indicated: $p < 0.05$ (*), $p < 0.01$ (**), and $p < 0.001$ (***).

RESULTS

*Na$_V$1.5 Expression in Cancer Cells and Role in Invasion in Vitro*—MDA-MB-231 breast cancer cells express transcripts for the cardiac Na$_V$1.5 isoform (Fig. 1*A*), which has been shown to be the only functional Na$_V$ α-subunit in these cells (16, 17, 26). Although it has been proposed that α-subunits alone are sufficient to form functional channels (27), mRNA for the β1, β2, and β4 auxiliary subunits are also expressed (Fig. 1*A*), suggesting that a complete Na$_V$ complex could exist, made up of an α-subunit associated with multiple auxiliary β-subunits. In all studied cells, voltage-dependent sodium currents were recorded. The mean current-voltage (I_{Na}-V) relationship of the sodium current is shown on Fig. 1*B* (n = 80 cells). The activation threshold takes place around -60 mV, and the maximal current density, obtained from a depolarizing pulse from -100 to -10 mV, is seen at -11.29 ± 0.89 pA/pF. Conductance-voltage and availability-voltage relationships show that at voltages between -60 and -20 mV, *i.e.* in the range of the membrane potentials of these cells ($E_m = -36.8 \pm 1.5$ mV; $n = 105$ cells), Na$_V$ are partially activated and not fully inactivated (Fig. 1*C*). This leads to a sustained "window" inward current at -30 mV, which is inhibited by 30 μM TTX (Fig. 1*D*). This sustained inward current can be increased by using the sodium channel opener veratridine (Fig. 2*A*). Blocking the sodium current with TTX decreased the invasiveness by about 40% (Fig. 2*B*). On the other hand, veratridine dose-dependently enhanced the invasiveness of MDA-MB-231 cells. TTX, veratridine (10 and 50 μM), and a mixture of both had no effect on cancer cell migration (supplemental Fig. S1*A*). To validate the influence of Na$^+$ entry on invasion through Na$_V$, the assays were repeated with decreasing the extracellular Na$^+$ concentration from 155 to 45
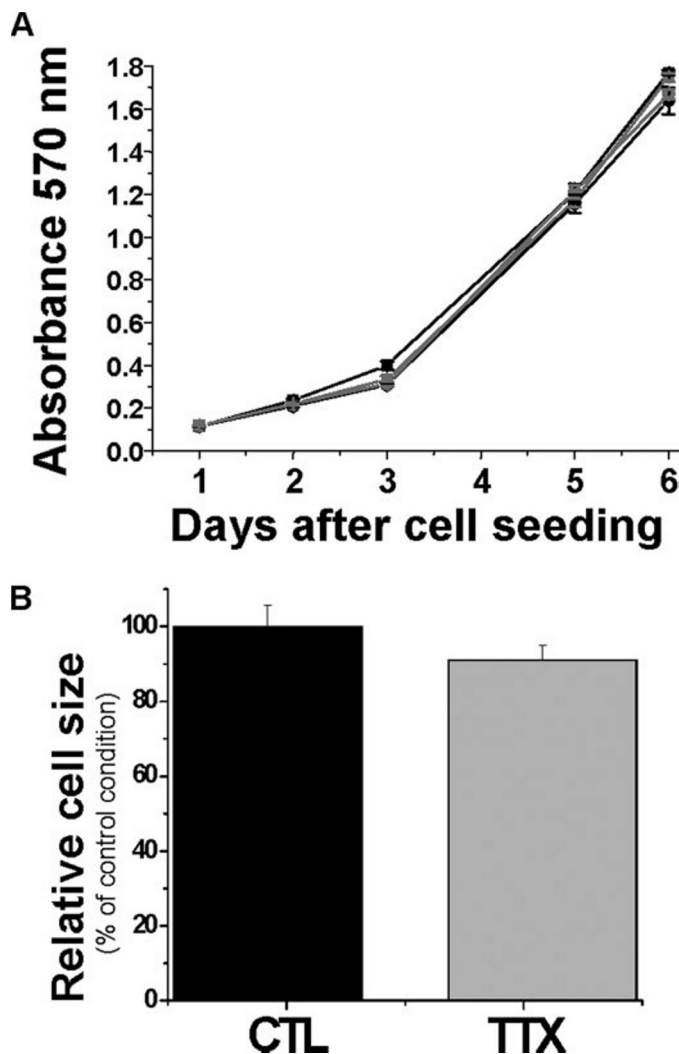

FIGURE 4. **Effect of Na$_V$ activity on MDA-MB-231 cell proliferation and colony growth.** *A*, cell growth for 6 days on noncoated (*squares*) and Matrigel®-coated (*circles*) 24-well plates, in presence (*gray*) or not (*black*) of 30 μM TTX, expressed as 570 nm absorbance. *B*, cell sizes were assessed using the ImageJ 1.38I software, in control (*CTL*, $n = 42$) or TTX conditions ($n = 42$).

mM (Fig. 2*C*). This resulted in a 3-fold reduction of I_{Na} (Fig. 2*C*, *panel a*) and a slight membrane potential hyperpolarization (-4.00 ± 1.62 mV, $n = 4$). Reducing the Na$^+$ concentration of the culture medium decreased invasion by ~34%, whereas it had no effect on cell viability for 24 h and no effect on Na$_V$1.5 expression (supplemental Fig. S2). Likewise, TTX was approximately three times less effective in reducing invasion in the Low Na$^+$ culture medium (Fig. 2*C*, *panel b*). This highlights the crucial role of the inward sodium gradient in cell invasion. We then knocked down the expression of Na$_V$1.5 by using a siRNA protocol (Fig. 3). The transfection of siRNA directed against Na$_V$1.5 mRNA was assessed by quantitative reverse transcription-PCR and resulted in a 65% reduction of expression compared with the transfection of siCTL (Fig. 3*A*). This reduction in mRNA level was associated to a ~70% reduction of the maximal current recorded when the cells were submitted to a depolarization from -100 to -5 mV (Fig. 3*B*). When Na$_V$1.5 expression was knocked

A

Cancer Cell Colony Growth and Three-dimensional Matrix Invasion—As we have previously reported, sodium channels promote cell invasion but do not participate in *in vitro* proliferation on non-coated culture dishes (15, 17) (Fig. 4A). Here, flasks were coated with a film of Matrigel® to evaluate its possible effect on cell proliferation. Cell proliferation as a monolayer on an extracellular matrix was not affected by the presence of TTX in the external medium, supporting the idea that cell proliferation did not depend on Na$_V$1.5 activity (Fig. 4A). Cell size was also unaffected by the TTX treatment (Fig. 4B). However, *in vivo*, cancer cells usually grow deep within a tissue, surrounded by extracellular matrix. To better mimic such conditions, the cells were spread into a three-dimensional Matrigel®-composed matrix. The day after seeding, the media were changed and replaced with control or TTX-containing media. Cell proliferation induced the formation of colonies with or without TTX (Fig. 5A). However, colonies were 56% smaller in the presence of TTX than in control conditions (Fig. 5B). Likewise, the number of cells escaping from the colonies and infiltrating the three-dimensional matrix was inhibited by 88% (Fig. 5C).

Proteolytic Activities of MDA-MB-231 Cells—Experiments were then performed to understand how Na$_V$1.5 function influenced the distribution of protease activity within the Matrigel®. To do so, we used DQ-gelatin, a gelatinic substrate that releases fluorescent products after proteolytic cleavage. As shown on Fig. 6A, the gelatinolytic activity is mainly distributed at the perimembrane level, which suggests that some gelatinases are released/secreted. Culture with TTX (30 μM) induced a weaker gelatinolysis at the cell periphery (~65% reduction of fluorescence intensity), supporting a regulatory role of Na$_V$ in extracellular gelatinolysis (Fig. 6). The fluorogenic substrate Z-FR-AMC (10 μM) was readily hydrolyzed by MDA-MB-231 cell lysates. Fluorescence release was almost 10 times higher at pH 5.5 than at pH 8.0 and was abolished by
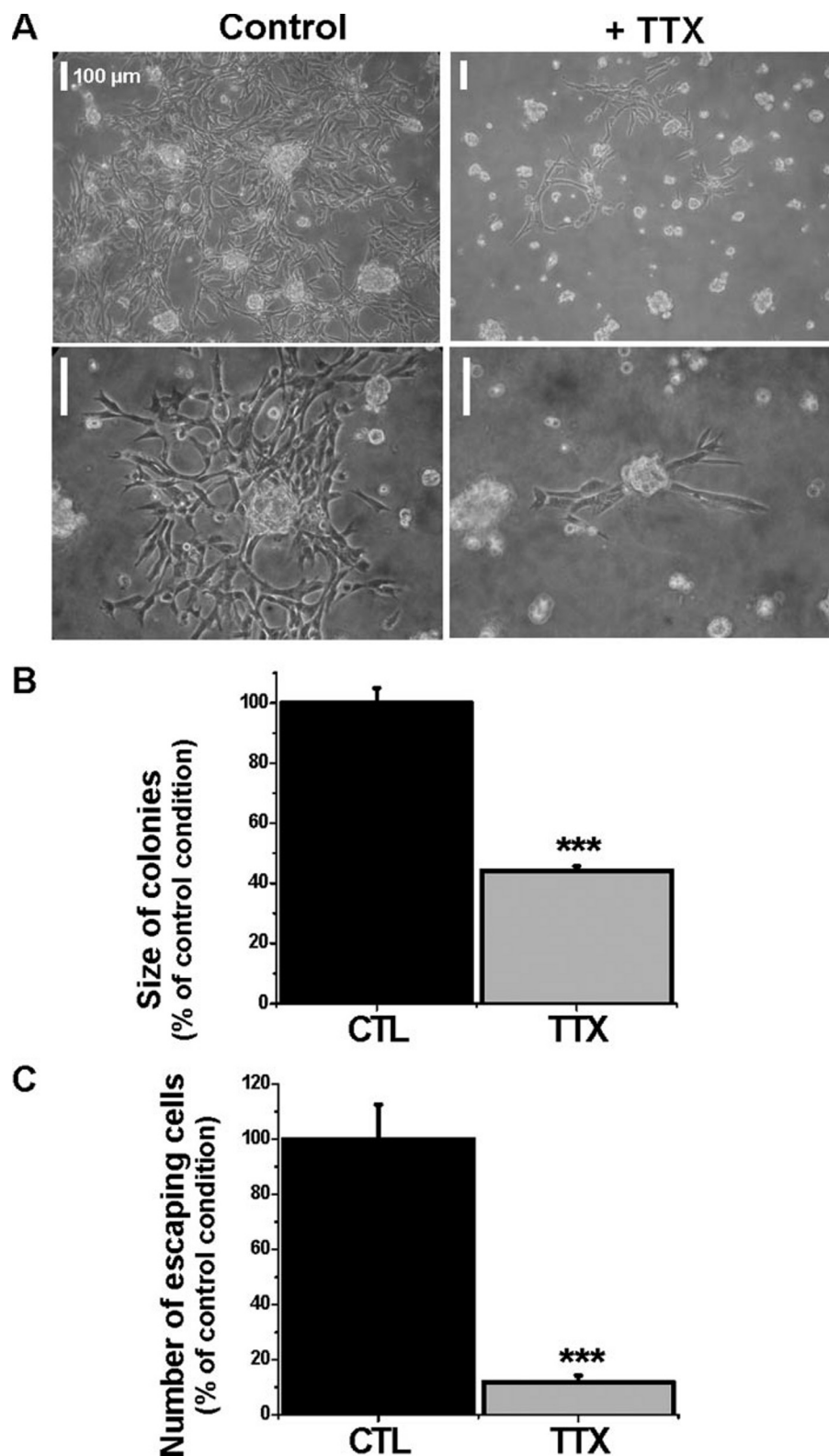
B

C

FIGURE 5. **Effect of Na$_V$ activity on MDA-MB-231 colony growth.** *A*, cancer cell colonies in a three-dimensional Matrigel® matrix in the presence or absence of 30 μM TTX. The pictures were taken with different objectives at the optical microscope: ×20 (*top pictures*) and ×40 (*bottom pictures*). The *scale bars* correspond to 100 μm. *B*, sizes of cancer cell colonies in control (*CTL, n* = 166) and TTX conditions (*n* = 274). *C,* number of cells escaping from colonies and invading the matrix were assessed in control (*n* = 2088) and TTX conditions (*n* = 245), using the ImageJ 1.38l software.

down, MDA-MB-231 cells invasiveness was reduced by about 35% and was no longer significantly reduced by TTX (Fig. 3C).
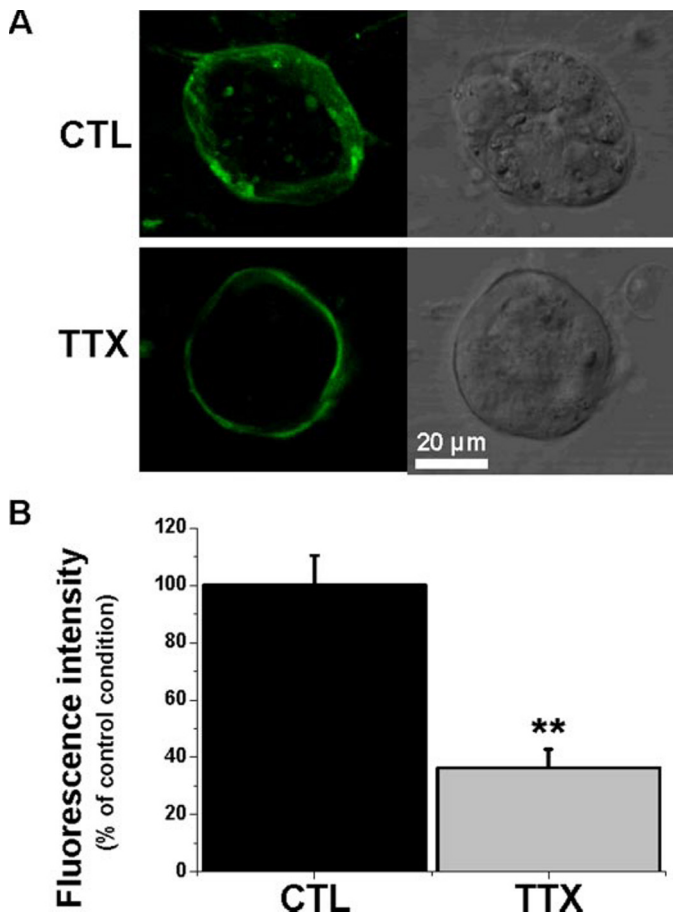
A

B

FIGURE 6. **Effect of Na$_V$ activity on MDA-MB-231 cells pericellular gelatinolysis.** *A*, confocal imaging of MDA-MB-231 cells grown for 24 h in a three-dimensional Matrigel® matrix containing DQ-Gelatin® in control conditions (*CTL*) or in presence of 30 μM TTX (TTX). The *scale bars* correspond to 20 μm. *B*, quantification of fluorescence intensity from DQ-gelatin cleavage in control conditions (*CTL*) or in presence of 30 μM TTX. **, $p < 0.01$ ($n = 3$).

addition of 100 μM E-64 (data not shown), indicating that hydrolysis was related to Cat activity and not to trypsin-like serine proteases. Cat activities were then measured in cell lysates using different specific substrates (Fig. 7*A*). In addition to Z-FR-AMC, which was degraded by all cysteine endopeptidases, cleavage of Z-RR-AMC indicated the presence of CatB. Z-LR-AMC was cleaved both at pH 5.5 (Fig. 7*A*) and under mild alkaline conditions (pH 7.5) after incubation for an hour (data not shown), indicating the presence of active CatS, which remains stable under such conditions in contrast to CatK (28–30).

Influence of Na$_V$ on Cathepsin-dependent Invasiveness of Cancer Cells—The relative contribution of Cat B, S, K, and L on cell invasiveness was investigated using combinations of specific cell-impermeant Cat inhibitors. CA-074, an inhibitor of CatB, reduced cell invasion by ~40% (Fig. 7*B*). The same reduction was observed with Z-FL-COCHO (CatS inhibitor). Z-L-NHNHCONHNH-LF-Boc (CatK inhibitor) reduced the invasion by ~25%, whereas *N*-(4-biphenylacetyl)-*S*-methylcysteine-(D)-Arg-Phe-β-phenethylamide (CatL inhibitor) had only a weak effect (<10%). Individual inhibition of CatB and S gave a similar reduction of invasion, so we further compared the effects of a mixture of both CA-074 and Z-FL-COCHO. In

that case, no significant additive effect was observed compared with their individual effects. Alternatively, submitting cells to a mixture of all given specific inhibitors (*i.e.* inhibitors for CatB, S, K, and L) reduced invasion by ~65%; this effect was the same as that observed with the broad spectrum Cat inhibitor E-64. This strongly suggests that CatB, S, K, and L are the main cysteine Cat involved in MDA-MB-231 cell invasion. Conversely, neither of the protease inhibitors tested had any effect on MDA-MB-231 cell survival/migration (supplemental Fig. S1, *B* and *C*).

The invasiveness of MDA-MB-231 cells was decreased by ~40 and ~65% in the presence of TTX and E-64, respectively (Fig. 7*C*). However, the combination of both TTX and E-64 did not further reduce cell invasion (~65%), compared with E-64 alone. These results indicate that Cat were mainly responsible for the Matrigel® degradation by MDA-MB-231 cells but also suggest that Na$_V$1.5 channels may partly promote Cat activities. Furthermore, TTX potentiated the inhibitory effects of CatK inhibitor (from 25 to 43%) on invasion, but not those of CatB, CatS, or CatL inhibitors. These results strongly support the idea that CatB-, CatS-, and CatL-mediated extracellular matrix degradation, but not that of CatK, is partially controlled by Na$_V$ activity. Because different isoforms of sodium channels have been reported to be involved in the invasion process of different cancer cell lines (15), we hypothesized that the link between Na$_V$ activity and invasion may occur through the modulation of Cat activities. We used the metastatic non-small cell lung cancer cell line H460, known to express TTX-sensitive sodium channels (18). E-64 inhibited ~75% of H460 cells invasion, indicating here again a prominent role of Cat in invasiveness (Fig. 7*D*).

To understand the mechanism by which Na$_V$ promotes CatB- and CatS-dependent invasiveness, we did quantitative PCR experiments to investigate whether the TTX treatment modified the mRNA expression of Cat or their physiological inhibitors, *i.e.* cystatins C and M and stefins A and B. Stefin A was very poorly expressed (data not shown), and therefore we focused on cystatins C and M and stefins B. TTX had no significant effect, neither on the mRNA expression of Cat as well as their inhibitors, nor on the expression of Na$_V$1.5 channels themselves (Fig. 8*A*). Because TTX induced a reduction of the extracellular degradation of DQ-gelatin (Fig. 6), we analyzed the effect of Na$_V$ on the membrane-associated and secreted forms of Cat. Titration experiments, performed on intact cells previously grown on Matrigel®, indicated that the concentration of active, membrane-associated Cat (total Cat as well as CatB) was not affected by the TTX treatment (Fig. 8*B*). Similarly, their concentrated cell-free supernatants showed comparable Cat activity toward Z-FR-AMC substrate at pH 5.5, in presence or not of TTX (Fig. 8*C*). Western blot analyses revealed the presence of mature single-chain (31 kDa), double-chain (25 kDa), and zymogen (45 kDa) forms of CatB (Fig. 7*D*) and mature (28 and 24 kDa) and proforms (36 kDa) of CatS. However, for both Cat, the mature forms were the predominant forms in cell lysates, whereas soluble proforms were predominant in cell-free supernatants. Densitometric analyses of CatB and S (proform and active forms) indicated that TTX had no effect, neither in cell lysates nor in supernatants, and therefore
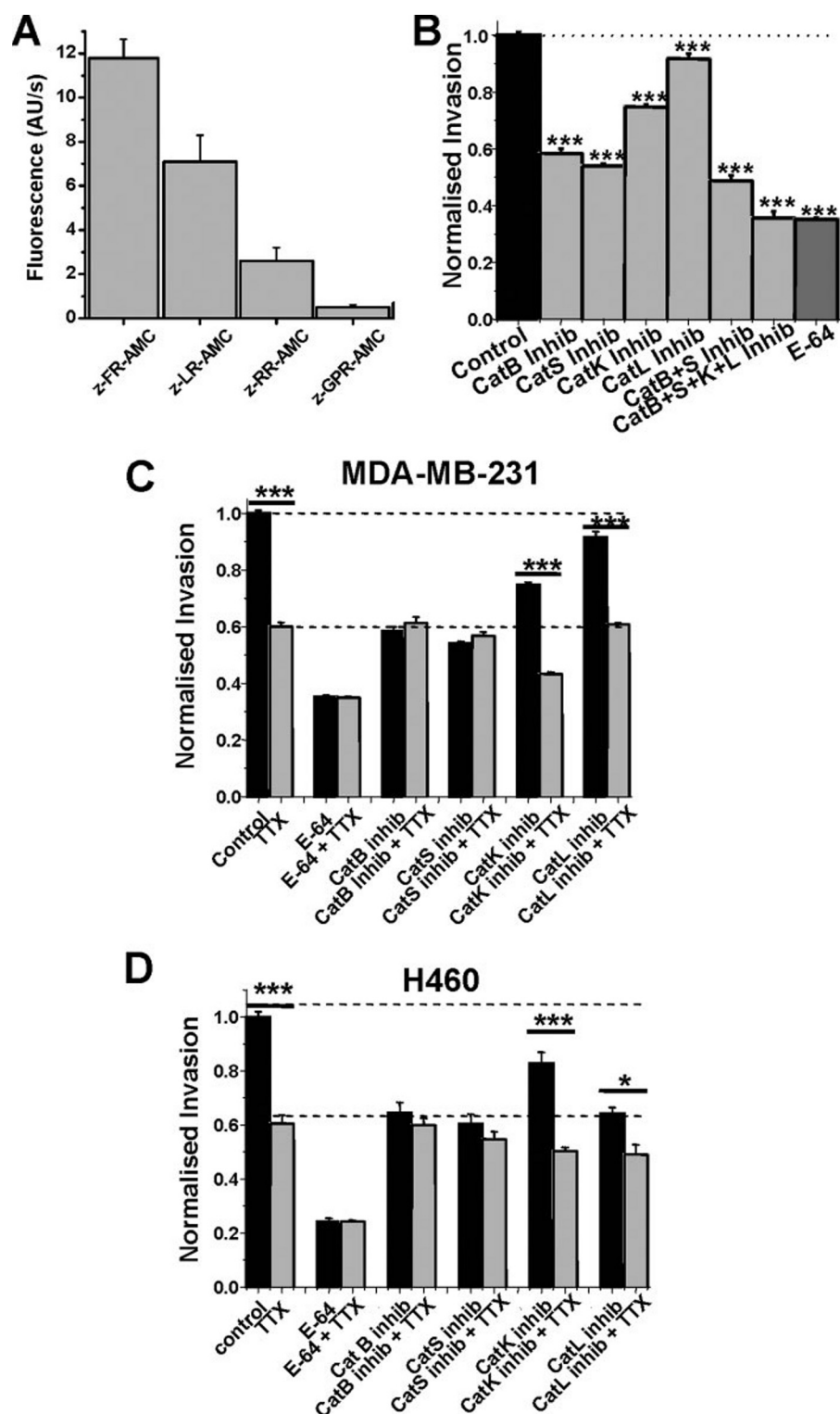
FIGURE 7. **Proteolytic activities in MDA-MB-231 cells: involvement of cathepsins in the invasion process.** *A*, enzymatic assays performed on total cell lysates (sodium-acetate buffer pH 5.5, 2 mM dithiothreitol, and 2 mM EDTA) in the presence of different fluorogenic substrates of Cat (see "Experimental Procedures") ($n = 4$ separate experiments). *B*, effect of specific or broad spectrum (E-64) Cat inhibitors on cell invasiveness. All the Cat inhibitors were responsible for a significant (***, $p < 0.001$) reduction of the cell invasiveness compared with the control condition ($n = 8$ separate experiments). *C*, effects of Cat inhibitors alone or in combination with 30 μM TTX on normalized Matrigel® invasion of MDA-MB-231 cancer cells ($n = 8$ separate experiments). *D*, effects of Cat inhibitors in presence or not of 3 μM TTX on Matrigel® invasion by H460 metastatic non-small cell lung cancer cells. Invasion through Matrigel® was normalized to the invasion in the absence of treatment (see "Experimental Procedures"). The effect of each inhibitor on invasion is compared with the same condition in presence of TTX. *, $p < 0.05$; ***, $p < 0.001$.

Na$_V$ inhibition did not affect CatB and S release (Fig. 8*D* and supplemental Fig. S3). Western blots were also performed for CatL and CatK; TTX had no effect on CatL amount in cell lysates or supernatants; CatK was immunodetected in cell lysates but not in supernatants (data not shown).

Cat are classically known to have an optimal activity in an acidic environment (7). We thus measured the intracellular and the perimembrane pH in control conditions or in presence of TTX (Fig. 9). The blockade of Na$_V$ activity with TTX led to an intracellular acidification (from pH 7.31 ± 0.03 to pH 6.87 ± 0.06; Fig. 9*A*), which was associated with a pericellular alkalinization (from pH 7.32 ± 0.03 to pH 7.47 ± 0.01; Fig. 9*B*) of MDA-MB-231 cancer cells. Na$_V$ activity is therefore responsible for the acidification of the perimembrane space.

DISCUSSION

Na$_V$1.5 (in the form of the fetal splice variant) have been shown to be expressed in the highly metastatic MDA-MB-231 breast cancer cells and in high grade cancer breast tissues but not in noncancer or low grade cancer biopsies (16, 17). Therefore Na$_V$ expression and functionality may be considered as markers of a metastatic phenotype. In the present study, we have identified molecular targets regulated by Na$_V$ activity and demonstrated their involvement in cancer cell invasiveness. This is the first attempt to determine the signaling pathway linking the function of ion channels in cancer cells with the regulation of proteolytic activity. Although Na$_V$ activity has no effect on the expression and secretion levels of Cat, it enhances their activity in the extracellular environment of breast cancer cells through the regulation of the perimembrane pH.

In a first part of this work, we showed that Na$_V$ were expressed and functional in highly invasive MDA-MB-231 breast cancer cells. Although the expression of Na$_V$ α-subunits is sufficient for channel
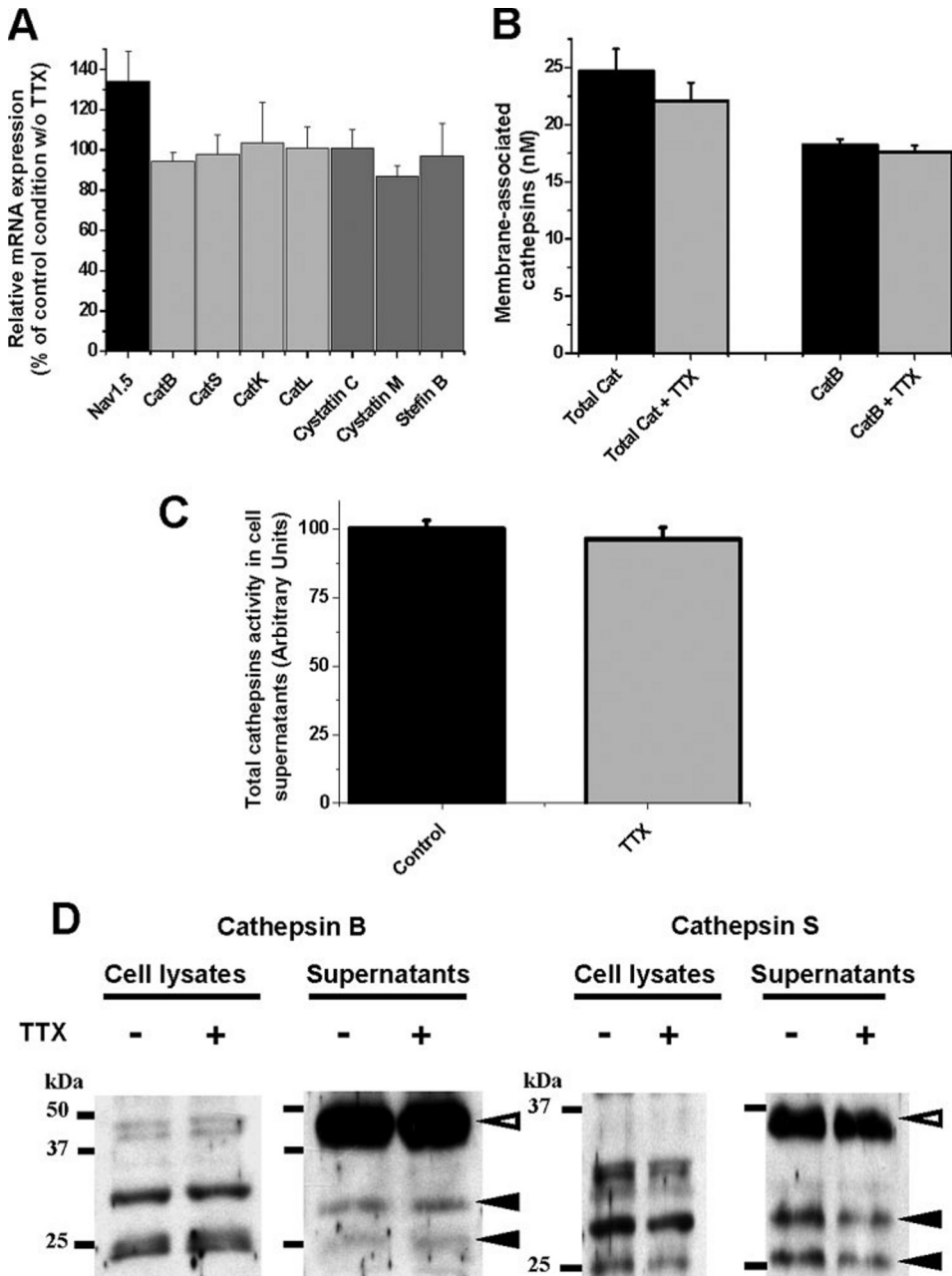
FIGURE 8. **Regulation of cathepsins by Na$_V$.** *A*, quantitative PCR showing the relative effect of the TTX treatment on the mRNA expression of Na$_V$1.5, Cat, and their physiological inhibitors. The results are expressed as percentages of control condition without TTX ($n = 4$ separate experiments). *B*, effect of TTX treatment on the membrane-associated Cat activity of intact cells. Cat titration was performed by using E-64. Alternatively, CA-074 was used to determine CatB concentration (see "Experimental Procedures") ($n = 6$ separate experiments). *C*, effect of TTX treatment on the Cat activity measured in concentrated supernatants (Buffer: 0.1 M sodium acetate, pH 5.5, containing 2 mM dithiothreitol, and 2 mM EDTA). Enzymatic assays were performed using Z-FR-AMC as a substrate ($n = 6$ separate experiments). *D*, Western blots for the Cat B and S in total cell lysates or in concentrated supernatants ($\times$100) from MDA-MB-231 grown for 24 h on Matrigel® in the presence or absence of 30 μM TTX. *White* and *black arrowheads* indicate proforms and mature Cat, respectively. These WB are representative of seven and four separate experiments for cathepsin B and S, respectively.

to restrain the expression of different Na$_V$ and associated proteins in excitable cells and demonstrated to be down-regulated or mutated in several cancers (32–34). Another interesting finding is the expression, in the p53-mutated MDA-MB-231 cells, of all the known β-subunits except β3 (SCN3B gene), which has been demonstrated to be a proapoptotic factor induced by p53 in cases of DNA damage (35).

We then demonstrated the presence of a continuous sodium influx (window current) through Na$_V$ at the membrane potential of the cancer cells. Blocking this residual channel activity with TTX, reducing the inward gradient of Na$^+$, or knocking down the expression of Na$_V$1.5 reduced cell invasiveness, while increasing channel opening with veratridine had the opposite effects. We thus propose that Na$_V$ exert their pro-invasive effects through the influx of sodium. We have previously shown that *in vitro* proliferation, as monolayers, was not affected by Na$_V$ activity (15). However, cancer cells *in vivo* are surrounded by other cells and connective tissues, making the proteolysis of the extracellular matrix a necessary process of tumor growth. Indeed even if Na$_V$ activity does not regulate cancer cell multiplication *per se*, it promotes tumor growth as a result of the extracellular matrix digestion. Here we have demonstrated that Na$_V$-regulated proteases allow cancer cells to spread and invade the surrounding matrix *in vitro*. We have shown that Na$_V$ functionality does not modulate cancer cell migration. This is in contradiction with what is observed by Djamgoz and co-workers (16), but we do not have any explanation for this apparent discrepancy (except for some different experimental conditions such as the use of migra-

functionality (31), auxiliary β-subunits are also expressed, and cancer cells express transcripts for complete Na$_V$ complexes. If the events leading to Na$_V$ expression in cancer cells are not known, it can be postulated that a transcription factor controlling the expression of a set of genes participating in ion channel function is deregulated. One candidate could be the transcription factor REST (RE-1 Silencing Transcription factor) known

tion inserts with 12-μm instead of 8-μm diameter pores and 10% instead of 5% fetal calf serum).

To digest the external matrix, cells express extracellularly active proteases that can be associated with the membrane but can also be released as soluble forms into the surrounding environment. This is confirmed by experiments using DQ-gelatin as a fluorescent substrate (36) (Fig. 6). We showed that Cat are
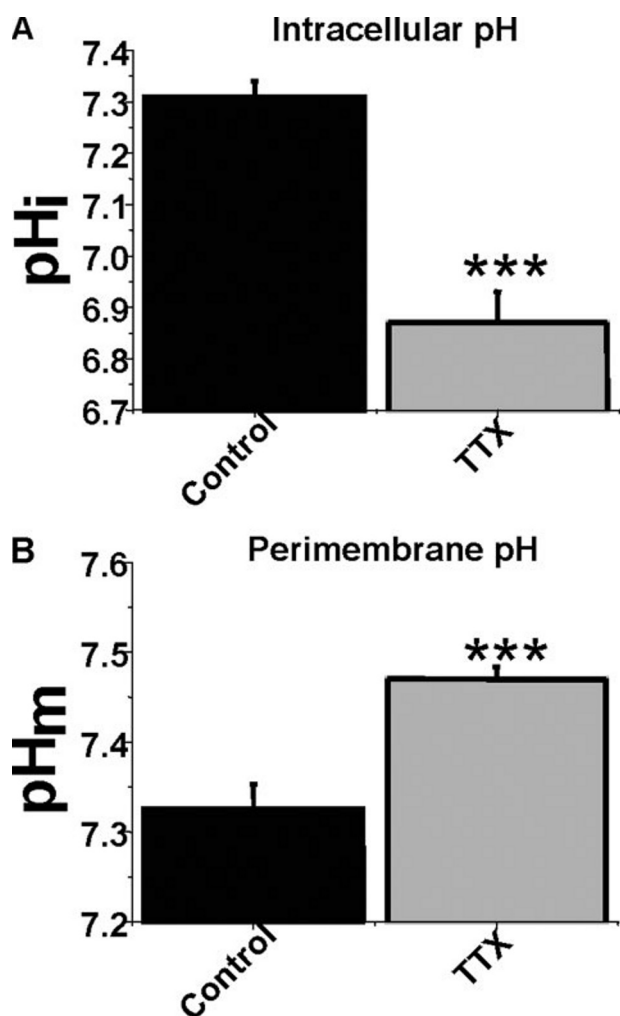
FIGURE 9. Regulation of internal and perimembrane pH by Na$_V$ activity. *A*, effect of TTX on intracellular pH (*pH$_i$*) measured using BCECF (*n* = 10 cells for TTX and *n* = 9 cells for control condition). *B*, effect of Na$_V$ activity on the perimembrane pH (*pH$_m$*) measured using the outer membrane leaflet pH-sensitive probe DHPE. ***, $p < 0.001$ (*n* = 8–10 cells).

predominantly responsible for MDA-MB-231 cancer cell invasiveness. The Cat involved are mainly CatB and CatS and are excreted/secreted to the extracellular medium.

Considering the fact that TTX does not have any additive effect on cell invasiveness when co-applied with CatL inhibitor, we could postulate that this cathepsin is regulated by Na$_V$ functioning. However, this reversible CatL inhibitor (*N*-(4-biphenylacetyl)-*S*-methylcysteine-(D)-Arg-Phe-β-phenethylamide) only leads to a weak inhibition of cell invasiveness (<10%), suggesting a very slight involvement in the extracellular matrix degradation. This apparent effect could also be due to a basal cross-reactivity with other, closely related enzymes.

In MDA-MB-231 cells, CatK was present in cell lysates (data not shown) but not immunodetected in supernatants, suggesting that it is restricted to intracellular compartments (lysosomes/endosomes). The effects of CatK inhibitor on cell invasiveness could therefore be attributed to nonspecific effects.

Because there is more and more evidence for the expression of functional Na$_V$ in metastatic cancer cell lines and tumors *in vivo* (15), we chose to study the invasiveness of the human lung cancer cell line H460, which also expresses functional Na$_V$ (18).

Here again we found that Cat are responsible for ~75% of cancer cell invasion (Fig. 7*D*). CatB, CatS, and CatL are involved in the invasion of H460 cells and are, at least partially, regulated by Na$_V$ activity. Although the ways in which Cat are secreted to the extracellular space are not completely understood, it is known in many different cancer types that they can be secreted as immature proforms as well as active forms (9). It has been reported that CatB can be released following the fusion of lysosomes with the plasma membrane (12). However, if this was the sole mechanism of release, we would only find mature forms (25 and 31 kDa, (37)) whereas we also identified a bigger quantity of proforms (45 kDa). Although Cat, such as CatS, are tightly regulated and can be auto-activated in the pericellular space at neutral pH, their optimal activity is obtained for acidic pH (7). We showed in this study that Na$_V$ tends to alkalinize intracellular pH, and acidify perimembrane extracellular pH, which renders the secreted Cat more active. In our experiments, because of proton diffusion, we probably underestimate the perimembrane acidification. The Na$_V$-dependent acidification might be greater in particular membrane locations, such as caveolae or podosome-like structures, leading to a specific microenvironment with a lower pH than observed globally. Indeed, the proteolytic activity is known to be concentrated in these particular perimembrane areas. Interestingly, a pericellular acidification of cancer cells has already been reported (38) and promotes metastasis in an *in vivo* model of human melanoma (39). The way by which Na$_V$ activity regulates intra- and extracellular pH is still unknown. It may involve regulation of different pH modulators such as the sodium-proton exchanger family (NHE), the bicarbonate transporter family (BCT), the vacuolar H$^+$-ATPase (V-ATPase), or the monocarboxylate transporter family (MCT). All of these pH regulators have already been proposed to be molecular targets for cancer chemotherapy (40, 41).

In conclusion, we showed herein that the abnormal expression of functional Na$_V$ complexes, known to be characteristic of highly metastatic cells, increases cell invasiveness and also increases cancer cell colony growth in three-dimensional matrices, through a pH-dependent, up-regulated Cat activity. In agreement with others (9, 10, 12, 42), we propose that cysteine Cat might be central players in cancer cell invasion, tumor growth and metastasis development. Na$_V$ activity results in the acidification of the perimembrane pH and thus enhances the proteolytic activity of Cat toward the surrounding matrix. We propose that the regulation of Cat involves the functionality of Na$_V$ and may be a general mechanism in highly aggressive cancers. Na$_V$ could be considered as new targets against tumor growth and metastases.

REFERENCES

1. Parkin, D. M., Bray, F., Ferlay, J., and Pisani, P. (2005) *CA-Cancer J. Clin.* **55,** 74–108

2. Baker, A. H., Edwards, D. R., and Murphy, G. (2002) *J. Cell Sci.* **115,** 3719–3727

3. Egeblad, M., and Werb, Z. (2002) *Nat. Rev. Cancer* **2,** 161–174

4. Turk, B. (2006) *Nat. Rev. Drug Discov.* **5,** 785–799

5. Turk, V., Turk, B., and Turk, D. (2001) *EMBO J.* **20,** 4629–4633

6. Chapman, H. A., Riese, R. J., and Shi, G. P. (1997) *Annu. Rev. Physiol.* **59,** 63–88

7. Lecaille, F., Kaleta, J., and Bromme, D. (2002) *Chem. Rev.* **102,** 4459–4488

8. Joyce, J. A., and Hanahan, D. (2004) *Cell Cycle* **3,** 1516–1619

9. Mohamed, M. M., and Sloane, B. F. (2006) *Nat. Rev. Cancer* **6,** 764–775

10. Gocheva, V., and Joyce, J. A. (2007) *Cell Cycle* **6,** 60–64

11. Punturieri, A., Filippov, S., Allen, E., Caras, I., Murray, R., Reddy, V., and Weiss, S. J. (2000) *J. Exp. Med.* **192,** 789–799

12. Roshy, S., Sloane, B. F., and Moin, K. (2003) *Cancer Metastasis Rev.* **22,** 271–286

13. Jane, D. T., Morvay, L., Dasilva, L., Cavallo-Medved, D., Sloane, B. F., and Dufresne, M. J. (2006) *Biol. Chem.* **387,** 223–234

14. Brix, K., Dunkhorst, A., Mayer, K., and Jordans, S. (2008) *Biochimie* (*Paris*) **90,** 194–207

15. Roger, S., Potier, M., Vandier, C., Besson, P., and Le Guennec, J. Y. (2006) *Curr. Pharm. Des.* **12,** 3681–3695

16. Fraser, S. P., Diss, J. K., Chioni, A. M., Mycielska, M. E., Pan, H., Yamaci, R. F., Pani, F., Siwy, Z., Krasowska, M., Grzywna, Z., Brackenbury, W. J., Theodorou, D., Koyuturk, M., Kaya, H., Battaloglu, E., De Bella, M. T., Slade, M. J., Tolhurst, R., Palmieri, C., Jiang, J., Latchman, D. S., Coombes, R. C., and Djamgoz, M. B. (2005) *Clin. Cancer Res.* **11,** 5381–5389

17. Roger, S., Besson, P., and Le Guennec, J. Y. (2003) *Biochim. Biophys. Acta* **1616,** 107–111

18. Roger, S., Rollin, J., Barascu, A., Besson, P., Raynal, P. I., Iochmann, S., Lei, M., Bougnoux, P., Gruel, Y., and Le Guennec, J. Y. (2007) *Int. J. Biochem. Cell Biol.* **39,** 774–786

19. Barrett, A. J., Kembhavi, A. A., Brown, M. A., Kirschke, H., Knight, C. G., Tamai, M., and Hanada, K. (1982) *Biochem. J.* **201,** 189–198

20. Towatari, T., Nikawa, T., Murata, M., Yokoo, C., Tamai, M., Hanada, K., and Katunuma, N. (1991) *FEBS Lett.* **280,** 311–315

21. Chowdhury, S. F., Sivaraman, J., Wang, J., Devanathan, G., Lachance, P., Qi, H., Menard, R., Lefebvre, J., Konishi, Y., Cygler, M., Sulea, T., and Purisima, E. O. (2002) *J. Med. Chem.* **45,** 5321–5329

22. Wang, D., Pechar, M., Li, W., Kopeckova, P., Bromme, D., and Kopecek, J. (2002) *Biochemistry* **41,** 8849–8859

23. Walker, B., Lynas, J. F., Meighan, M. A., and Bromme, D. (2000) *Biochem. Biophys. Res. Commun.* **275,** 401–405

24. Mosmann, T. (1983) *J. Immunol. Methods* **65,** 55–63

25. Laemmli, U. K. (1970) *Nature* **227,** 680–685

26. Jude, S., Roger, S., Martel, E., Besson, P., Richard, S., Bougnoux, P., Champeroux, P., and Le Guennec, J. Y. (2006) *Prog. Biophys. Mol. Biol.* **90,** 299–325

27. Catterall, W. A. (1986) *Annu. Rev. Biochem.* **55,** 953–985

28. Serveau-Avesque, C., Martino, M. F., Herve-Grepinet, V., Hazouard, E., Gauthier, F., Diot, E., and Lalmanach, G. (2006) *Biol. Cell* **98,** 15–22

29. Bromme, D., Steinert, A., Friebe, S., Fittkau, S., Wiederanders, B., and Kirschke, H. (1989) *Biochem. J.* **264,** 475–481

30. Vasiljeva, O., Dolinar, M., Pungercar, J. R., Turk, V., and Turk, B. (2005) *FEBS Lett.* **579,** 1285–1290

31. Catterall, W. A. (2000) *Neuron* **26,** 13–25

32. Coulson, J. M., Edgson, J. L., Woll, P. J., and Quinn, J. P. (2000) *Cancer Res.* **60,** 1840–1844

33. Lawinger, P., Venugopal, R., Guo, Z. S., Immaneni, A., Sengupta, D., Lu, W., Rastelli, L., Marin Dias Carneiro, A., Levin, V., Fuller, G. N., Echelard, Y., and Majumder, S. (2000) *Nat. Med.* **6,** 826–831

34. Westbrook, T. F., Martin, E. S., Schlabach, M. R., Leng, Y., Liang, A. C., Feng, B., Zhao, J. J., Roberts, T. M., Mandel, G., Hannon, G. J., Depinho, R. A., Chin, L., and Elledge, S. J. (2005) *Cell* **121,** 837–848

35. Adachi, K., Toyota, M., Sasaki, Y., Yamashita, T., Ishida, S., Ohe-Toyota, M., Maruyama, R., Hinoda, Y., Saito, T., Imai, K., Kudo, R., and Tokino, T. (2004) *Oncogene* **23,** 7791–7798

36. Mook, O. R., Van Overbeek, C., Ackema, E. G., Van Maldegem, F., and Frederiks, W. M. (2003) *J. Histochem. Cytochem.* **51,** 821–829

37. Linebaugh, B. E., Sameni, M., Day, N. A., Sloane, B. F., and Keppler, D. (1999) *Eur. J. Biochem.* **264,** 100–109

38. Bourguignon, L. Y., Singleton, P. A., Diedrich, F., Stern, R., and Gilad, E. (2004) *J. Biol. Chem.* **279,** 26991–27007

39. Rofstad, E. K., Mathiesen, B., Kindem, K., and Galappathi, K. (2006) *Cancer Res.* **66,** 6699–6707

40. Izumi, H., Torigoe, T., Ishiguchi, H., Uramoto, H., Yoshida, Y., Tanabe, M., Ise, T., Murakami, T., Yoshida, T., Nomoto, M., and Kohno, K. (2003) *Cancer Treat. Rev.* **29,** 541–549

41. Sennoune, S. R., Bakunts, K., Martinez, G. M., Chua-Tuan, J. L., Kebir, Y., Attaya, M. N., and Martinez-Zaguilan, R. (2004) *Am. J. Physiol.* **286,** C1443–C1452

42. Joyce, J. A., Baruch, A., Chehade, K., Meyer-Morse, N., Giraudo, E., Tsai, F. Y., Greenbaum, D. C., Hager, J. H., Bogyo, M., and Hanahan, D. (2004) *Cancer Cell* **5,** 443–453